Chemical Reaction Initiation and Hot-Spot Formation in Shocked Energetic Molecular Materials

A. Tokmakoff and M. D. Fayer*

Department of Chemistry, Stanford University, Stanford, California 94305

Dana D. Dlott

School of Chemical Sciences, University of Illinois at Urbana—Champaign, Urbana, Illinois 61801

Received: September 22, 1992; In Final Form: December 10, 1992

A theoretical model is developed to describe the nature of molecular energy transfer and chemical reactivity in shocked energetic materials. The intent is to develop a fundamental understanding of the sensitivity of secondary explosives, which are solids consisting of large organic molecules. Because secondary explosives are stable molecules with large barriers to chemical reaction, before reactions can occur, a sizable amount of energy must be transferred from the shock produced phonons to the molecules' internal vibrations by multiphonon up-pumping. The dominant mechanism for up-pumping is anharmonic coupling of excited phonon modes with low frequency molecular vibrations, termed doorway modes. Quantitative calculations are presented which show the extent and rate of multiphonon up-pumping caused by shock excitation. A simple expression is derived to describe how the rate of up-pumping increases with shock pressure. It is shown that up-pumping is complete, and Arrhenius kinetics become valid, within ~30 ps or 100–170 nm behind the shock front. The time dependence of chemical reactivity behind the front is calculated using reaction rate laws for the decomposition of nitramine explosives. The sensitivity of explosives is examined under the conditions of greatest interest: the regime of relatively weak shock waves (p = 1–10 GPa) characteristic of accidents. A mechanism for hot spot formation, based on defect induced local increases in anharmonic coupling, is discussed, and the conditions for ignition and spreading of reactions from hot spots are evaluated.

I. Introduction

Shock-initiated molecular reactions require transfer of substantial amounts of mechanical energy from the shock front to the internal vibrational states of the molecules.[1-6] This process is termed multiphonon up-pumping. The energy from the shock deposited in the external phonon modes is transferred to the internal vibrational degrees of freedom of a molecule, heating them to a temperature at which a chemical bond can be broken. The dynamics in this type of system involve the complex interplay of phenomena operating on a variety of time and distance scales. Elucidating the short time dynanics presents a severe test of our fundamental knowledge of solid state processes, especially the coupling between internal and external modes in molecular solids.

A specific motivation for trying to understand the behavior of molecular materials behind a shock front is the problem of *explosive sensitivity*. Sensitivity refers to explosive phenomena caused by perturbations which are ordinarily insufficient to produce a detonation.[7] During the detonation of an explosive solid, the thermodynamic state of the system is accurately described by the Chapman–Jouguet (CJ) model.[8-12] However, this successful theory does not provide insight into the molecular level events occurring in the solid behind the shock front. One likely place to look for conditions which promote sensitivity is the zone of highly nonequilibrium conditions just behind the front. In the past, attempts have been made to broaden the CJ theory to account for various intermediate zones which lie between the unreacted solid and the reaction products, e.g., the Zel'dovich–von Neumann–Doering (ZND) model[13] and the nonequilibrium ZND model.[11] However, a significant obstacle to understanding shock initiation of chemical reactions has been the general lack of fundamental understanding of molecular level mechanical energy transfer processes near the shock front.

During the 1980s, several authors recognized the importance of multiphonon up-pumping in energetic materials, and attempts were made to calculate the rate of vibrational up-pumping in nitromethane and in nitramines such as RDX.[1,3,14] The time scales calculated by these authors for the excitation of molecular vibrations by shock induced up-pumping were surprisingly long, ranging from a few tens of ns[3] to hundreds of ns.[14] The inefficiency of up-pumping was attributed to the large gap between the highest phonon frequency and the frequency of molecular vibrations. This gap necessitated a high-order multiphonon pump mechanism. These treatments gave rise to much speculation about the relationship between proposed "vibration-starved" molecules behind the front and various experimental observations, such as the rather slow reaction rate constant for the overall formation of the detonation products,[1,15] and the induction period which precedes detonation.[14]

In contrast, recent experimental studies of the flow of vibrational energy into or out of large organic molecular solids showed that these processes were far more efficient than predicted previously. In fact, they occur on the 10 to 100 ps time scale.[5,16-19] For example, a recent measurement of multiphonon up-pumping in nitromethane at 0.2 GPa and 300 K showed that up-pumping of both the C–N bend and the C–N stretching modes occurs in about 100 ps.[16] Other studies on molecular crystals, principally on the model system naphthalene, have revealed the existence of a mechanism for up-pumping[5,18,19] which is much more efficient than the high-order processes considered previously. It was shown that the relatively low-frequency, large-amplitude vibrations in large molecules can be excited readily via a low order anharmonic coupling process, typically two-phonon absorption. Once these vibrations, termed *doorway modes*, become excited, a variety of efficient intramolecular vibrational redistribution (IVR) processes come into play, redistributing energy from the excited doorway modes to the other internal vibrations. A fundamental conclusion of these studies is that multiphonon up-pumping occurs on a tens of picosecond time scale, approximately at the rate of doorway mode excitation, and, owing to efficient IVR processes, the internal vibrational states of up-pumped molecules are unlikely to deviate much from a thermal (Boltzmann) population distribution.[5,16,20]

In an earlier report, the anharmonic doorway mode model was used to describe multiphonon up-pumping behind a shock front

0022-3654/93/2097-1901$04.00/0

and the initiation of chemical reactions of energetic materials in the bulk and in the vicinity of a defect site.[5] The study presented here significantly expands on the previous work by accounting for a number of important features, including pressure effects on the rate of up-pumping and chemical reactions, the irreversible nature of shock wave heating, and the description of various nonequilibrium zones produced just behind the shock front.

It is the intent of this paper to use this model to examine the critical aspects of the sensitivity of secondary explosives. Unlike primary explosives, which are small unstable molecules with low barriers to reaction, the secondary explosives are relatively stable molecular solids with high barriers to reaction. Thus, the problem of explosive sensitivity assumes the greatest importance when the shock is relatively weak ($P < 10$ GPa). A considerable simplification is achieved by restricting the model to the investigation of processes occurring in the wake of relatively weak shocks through solids composed of large organic molecules. For a relatively weak shock, material behind the shock front is compressed and heated, but hydrodynamic phenomena, which can produce major physical and chemical alterations of the material, are unimportant.

Most secondary explosives consist of large organic molecules, e.g., HMX, RDX, TNT, TATB, PETN, and NTO (HMX = 1,3,5,7-tetranitro-1,3,5,7-tetraazacyclooctane, RDX = 1,3,5-trinitro-1,3,5-triazacyclohexane, TNT = 2,4,6-trinitrotoluene, TATB = 1,3,5-triamino-2,4,6-trinitrobenzene, PETN = pentaerythritol tetranitrate, and NTO = 3-nitro-1,2,4-triazol-5-one). Although detonations of large single crystals have been studied to a limited extent,[21] widely used energetic materials are generally formulations of molecular crystallites in polymer binders. The specific system begin considered here, HMX, is present in many common explosives and propellants. One of the most thoroughly studied energetic materials, PBX 9404,[22] for which an extensive data base exists, consists of 94% HMX in nitrocellulose.

Figure 1 is a schematic representation of the essential elements of a shock wave as described by the model calculations. Figure 1a shows an idealized shock front propagating through a material whose initial state is characterized by a pressure P_0, a temperature T_0, and a specific volume V_0, and whose final state is characterized by P_1, T_1, and V_1. The choice of three parameters to define the equation of state for the solid is purely arbitrary, and can also be replaced with convenient parameters such as the shock velocity U_s, the mass velocity U_p, or the compression ratio V_1/V_0. The pressure–volume relationship for a shocked solid, the Hugoniot, gives the final state of a shocked solid with a knowledge of the initial state, P_0 and V_0, in addition to a third variable characteristic of the shock wave, such as P_1, V_1, U_s, and U_p.

Figure 1b shows the essential physical and chemical elements of the shock wave as described by the model.[10] The shock front has a finite rise time, in which the mechanical energy of the shock is transferred to and equilibrates among the phonon modes. Typically the rise of the front extends over a few nm, corresponding to a rise time of ~ 1 ps.[1,4] In this phonon-rich zone the molecular vibrations, which are not directly pumped by the shock, have yet to be excited. In the up-pumping zone, the energy in the phonon modes is transferred to the vibrations by multiphonon up-pumping processes, and the two baths equilibrate within $\sim 10^{-10}$ s (10^{-7} m). As the vibrational modes are excited, reactivity is enhanced and bond breaking due to thermal decomposition occurs in the molecules. This is the ignition zone and extends to $\sim 10^{-9}$ s (10^{-6} m) behind the shock front. In energetic materials, endothermic bond breaking reactions are the precursors to detonation, a series of exothermic chain reactions occurring in a reaction zone 10^{-8}–10^{-6} s (10^{-5}–10^{-3} m) behind the front.[10,23]

The model presented below describes the dynamics of the processes behind the shock front in terms of quasitemperatures θ. A quasitemperature is used to characterize the state of a particular collection of degrees of freedom in a situation in which the entire system is not in thermal equilibrium. Initially, the phonon and vibrational quasitemperatures are equilibrated at

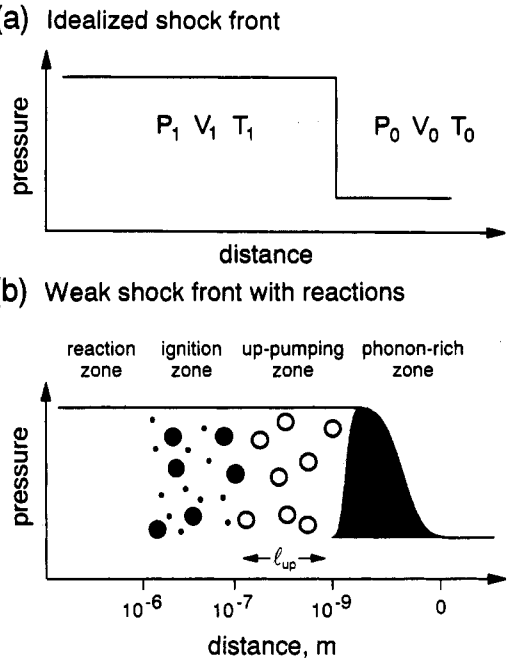

Figure 1. Diagram for shock wave propagation. (a) An idealized shock front propagating at velocity U_s into a medium with pressure P_0, specific volume V_0, and temperature T_0. The equivalent parameters behind the front are P_1, V_1, and T_1. (b) A schematic illustration of the features of the model. The shock front has a finite width and a phonon-rich zone immediately behind the leading edge. Following the front is the up-pumping zone of width l_{up}, where molecular vibrations are pumped by phonons. Hot spots can form around defect perturbed domains in this zone. The chemical reaction probability is greater at the hot spots than in the bulk. In the ignition zone, a reacted hot spot of sufficient size can cause a reaction to spread through the bulk. An isolated reacted bulk molecule cannot. If ignition occurs, a reaction zone is formed behind the ignition zone.

the ambient temperature, $\theta_{ph} = \theta_{vib} = T_0$. At $t = 0$ the shock is applied and the mechanical energy is quickly deposited exclusively in the external modes and redistributed among all the phonons. This corresponds to an initial condition where the phonon quasitemperature $\theta_{ph}(0) \gg T_0$, but the vibrational quasitemperature $\theta_{vib}(0) = T_0$. In the up-pumping zone, θ_{vib} increases while θ_{ph} decreases, leading to an eventual equilibration of internal and external degrees of freedom at $\theta_{ph} = \theta_{vib} = T_1$.

Because of the rapid increase in θ_{vib} in the up-pumping zone, the chemical reactivity of the shocked solid increases dramatically. Initial reactions will involve endothermic, unimolecular bond cleavage to form a variety of reactive species. For example, the first step in HMX solid-state decomposition is thought to involve loss of NO_2 through N–N bond cleavage.[24] Endothermic reactions alone cannot ignite or spread through the material. Ignition requires highly exothermic reactions which produce heat faster than it is dissipated by conduction, leading to chain reactions occurring on a 10^{-9}–10^{-6}-s time scale.[10] In secondary explosives, a series of overall endothermic steps are required before any heat generation is possible. These steps lead to the production of "fuel" molecules. It is the *bimolecular* reactions of these fuel molecules which release significant amounts of heat. In nitramines, such as HMX, the most important fuel reactions are $H_2CO + NO_2$ and $HCN + HONO$.[25] Clearly, significant release of chemical energy demands a large local concentration of fuel molecules. With weak shocks, the probability of a chemical reaction occurring in the bulk material is small, and reacted molecules are isolated from each other. Under these circumstances, ignition cannot occur.

It has been suggested by many workers that subthreshold ignition of energetic materials involves the generation of hot spots.[1,26,27] Although the actual mechanism of hot spot formation has not been experimentally determined, a variety of mechanisms have been proposed for the formation of hot spots, including

adiabatic compression of trapped gas in voids, friction involving sliding or impacting surfaces, shear band formation caused by mechanical failure, sparks, triboluminescence, and heating at crack tips.[21,28-30]

The presence of conditions far from equilibrium in the up-pumping zone suggests a fundamentally new mechanism for the formation of hot spots that does not require material failure or plastic deformation. The presence of defects in the up-pumping zone can lead to a local increase in the anharmonic coupling between the hot phonon bath and the molecular doorway modes.[5] The increased anharmonic coupling enhances the effects of up-pumping in a defect-perturbed domain (DPD), which may be larger than the defect itself.[31,32] This leads to the formation of a transient hot spot behind the front, by causing the DPD vibrational quasitemperature, θ_d, to momentarily over shoot the final temperature, T_1. Since the likelihood of a bond-breaking reaction is highly sensitive to the vibrational quasitemperature, a concentrated cluster of reacting and reacted molecules can be formed near the defect. The local high concentration of initial reactions and reaction products provides ideal conditions for the onset of exothermic reactions. Whether the reaction spreads or dies out depends on the peak temperature and size of the hot spot.[30,33,34] The DPDs, which have elevated vibrational quasitemperatures, a high concentration of reacted molecules, and a volume greater than the defect itself, can form hot spots which lead to ignition. Individual molecules outside a DPD may react; however, under relatively weak shock conditions, the presence of these scattered reaction sites does not favor exothermic reactions, and they are too small to ignite the surroundings.

In this paper, we present quantitative calculations based on a model of the processes described briefly above. The results lead to straightforward predictions regarding the structure of the nonequilibrium layers behind the front and the conditions required for ignition. The multiphonon up-pumping rate is calculated, and its pressure dependence is obtained. The time-dependent molecular vibrational quasitemperature is used to calculate the time dependence of the chemical reaction probability and its pressure dependence. The mechanism for anharmonic defect hot spot formation is introduced, the time dependence of up-pumping at DPDs is calculated, and the influence of hot spot formation on chemical reactivity is demonstrated. The width of the various zones shown in Figure 1b are determined, and the pressure dependence of shock initiation and the applicability of Arrhenius kinetics are considered.

To perform these calculations, a knowledge of a number of thermodynamic and kinetic parameters is required. Molecular materials have not been studied as extensively as simpler materials, however, the thermodynamic parameters, spectroscopic data, and ultrafast time-resolved mechanical energy transfer measurements required for the calculations are available for naphthalene, the prototypical molecular crystal.[35,36] The shock Hugoniot is not known for naphthalene, but it is available for the closely related substance, anthracene.[37,38] Since naphthalene is not an energetic material, chemical reactivity was incorporated into the model using thermal decomposition data obtained for HMX,[39,40] which has a similar crystal structure.[41] Although a mix of parameters from naphthalene, anthracene, and HMX are used, the nature of the effects and trends will be correct, and the results of the calculations will be essentially quantitative.

II. Multiphonon Up-Pumping in the Bulk Material

(A) Multiphonon Up-Pumping Model. Immediately behind the shock front, molecules with cold internal vibrations are immersed in a bath of highly excited phonons. Up-pumping into the internal vibrational modes is predominately through doorway modes. Doorway modes are molecular vibrations located just above the phonon cutoff frequency Ω_{max}, as shown in Figure 2. The large molecules being considered, naphthalene and HMX, have doorway modes whose frequency Ω is in the range $\Omega_{max} \leq \Omega \leq 2\Omega_{max}$. Therefore doorway mode pumping in these systems occurs via simultaneous absorption of two phonons. Absorption of further phonons transfers energy into higher modes until the IVR threshold energy (ΔE_{IVR}) is reached, as shown in Figure 2a. Once ΔE_{IVR} is reached, IVR randomizes the excitation. If doorway mode pumping is much more efficient than energy transfer from doorway modes to other low frequency vibrations, then doorway mode overtones are pumped by the shock up to ΔE_{IVR}, as shown in Figure 2b. In addition, HMX has very low frequency vibrational modes involving NO_2 rocking motions which lie below Ω_{max}.[42] These vibrations do not act as doorway modes because they are amalgamated with the phonons as in Figure 2c.[43-45] Amalgamated vibrations behave much like phonons in that they will be directly excited by the shock. In this case, the rate-limiting step in pumping the other molecular vibrations is energy transfer from the amalgamated phonon bath to the doorway modes, i.e., the vibrations just above Ω_{max}.

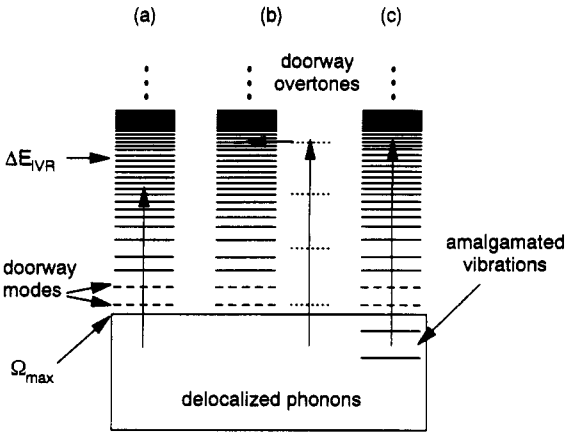

Figure 2. Schematic energy level diagram for doorway mode pumping by delocalized phonons produced by the shock, with phonon frequencies ranging from 0 to Ω_{max}. (a) Doorway modes are molecular vibrations located just above Ω_{max}. In naphthalene, doorway modes are pumped by two-phonon absorption. Energy is transferred out of the doorway modes into the other molecular vibrations by absorption of more phonons until an amount of energy ΔE_{IVR} is absorbed. Then efficient intramolecular vibrational redistribution processes further assist the randomization of intramolecular energy. (b) For highly efficient doorway mode pumping, doorway mode overtones are pumped by the shock up to ΔE_{IVR}, and then IVR randomizes the excitation. (c) In HMX and other nitramines, low frequency NO_2 torsions are amalgamated into the phonons and are directly pumped by the shock. Then energy transfer from the amalgamated phonons to the doorway modes just above Ω_{max} is the rate-limiting step in up-pumping.

The dominance of doorway mode up-pumping is attributed to two factors. First, owing to the large amplitude and low frequency of the doorway modes, they are the most highly anharmonic of all the internal vibrations. Second, the efficiency of a phonon pumping process decreases rapidly with the order of the process, i.e., the number of phonons simultaneously absorbed.[46] Doorway mode pumping requires absorbing the fewest phonons, and is thus the most efficient way to transfer energy from external to internal modes.

Once doorway modes become excited, a variety of IVR processes rapidly redistribute the vibrational energy among the various other internal modes.[47] This produces a vibrational distribution which is essentially in internal equilibrium.[16,20,48] In Figure 2a, which represents the case of naphthalene,[49] doorway mode pumping followed by absorption of additional phonons, one phonon at a time, excites the lower energy molecular vibrations. When the amount of internal energy becomes comparable to the naphthalene IVR threshold energy $\Delta E_{IVR} \approx 2200$ cm^{-1},[50] additional IVR processes, not requiring phonons, come into play, further assisting the thermalization of the internal vibrations.

The anharmonic term in the potential which causes doorway mode pumping is a cubic term of the form[46,49]

$$V^{(3)} = \frac{1}{3!}\sum_{\Psi}\frac{\partial^3 V(\{\Psi\})}{\partial\Psi_1\partial\Psi_2\partial\Psi_3}\Big|_{\{\Psi\}_0}\Psi_1\Psi_2\Psi_3 \quad (1)$$

Here $V(\{\Psi\})$ is the potential energy surface for the molecular crystal with a set of normal coordinates $\{\Psi\}$, and the partial derivative is evaluated at the equilibrium position $\{\Psi\}_0$. The cubic anharmonic term gives rise to thermal expansion,[51] and a variety of three-phonon processes involving two-phonon absorption, spontaneous and stimulated emission. The most efficient route for doorway mode pumping is absorption of a pair of phonons whose frequencies are about one-half the doorway mode frequency Ω.[5,43,48] The temperature and specific-volume dependent rate constant for energy transfer between a doorway mode of frequency Ω, and a pair of phonons whose frequencies lie near $\Omega/2$ is[5,46,52-54]

$$k_{2ph\rightarrow vib} = \frac{36\pi^2}{\hbar}\langle V^{(3)}(V)\rangle^2\rho^{(2)}(\Omega)[n_{ph}(T,V) - n_{vib}(T,V)] \quad (2)$$

Here $\langle V^{(3)}(V)\rangle$ denotes the specific volume-dependent matrix element of the operator in eq 1, $\rho^{(2)}(\Omega)$ is the two-phonon density of states at the doorway mode frequency Ω. Also, $n_{ph}(T,V)$ refers to the Planck occupation factor of phonons of frequency $\omega = \Omega/2$, $n_{ph}(T,V) = \{\exp(\hbar\omega(V)/k_BT) - 1\}^{-1}$, and $n_{vib}(T,V)$ is the Planck occupation factor at the doorway mode frequency Ω.

The value of $\langle V^{(3)}(V)\rangle$ can be determined empirically, or by direct calculation using model intramolecular potentials.[53,54] Measurement of vibrational relaxation processes of the form $k_{vib\rightarrow 2ph}$,[52] which can be related to $k_{2ph\rightarrow vib}$ by microscopic reversibility,[5] can be made using ps time-resolved spectroscopy, or high resolution vibrational spectroscopy, provided that energy relaxation is the dominant line broadening process. That is the case for pure crystals at low temperature,[19] but not necessarily the case at ambient temperature. (It should be noted that similar arguments have been used to calculate the up-pumping rate of nitromethane from the ambient temperature infrared spectrum.[3] However vibrational line broadening in liquids is not dominated by vibrational energy relaxation processes, but rather by pure dephasing.[55]) The phonon density of states is known for many materials, including naphthalene,[46] so $\langle V^{(3)}(V)\rangle$ can be determined from vibrational relaxation measurements using eq 2.[18,19]

At the temperatures being considered, the Planck occupation factors $n_\omega(T)$ can be approximated as $n_\omega(T) \approx k_BT/\hbar\omega$. Therefore, the up-pumping rate is proportional to the difference in quasitemperatures, that is $n_{ph}(T) - n_{vib}(T) \propto (\theta_{ph} - \theta_{vib})$.[5,48] Then the time dependence of the phonon and vibrational quasitemperatures can be described by the differential equations[5]

$$\frac{\partial\theta_{ph}}{\partial t} = \frac{\kappa(V)}{C_{p,ph}}[\theta_{vib} - \theta_{ph}] \quad (3a)$$

$$\frac{\partial\theta_{vib}}{\partial t} = \frac{\kappa(V)}{C_{p,vib}(\theta_{vib})}[\theta_{ph} - \theta_{vib}] \quad (3b)$$

where the constant pressure heat capacity of the vibrational modes, $C_{p,vib}(\theta_{vib})$, is dependent on the vibrational quasitemperature. In eqs 3, the parameter $\kappa(V)$ is the specific volume-dependent energy transfer parameter, which characterizes the rate of flow between phonons and vibrations.

A solution to eqs 3 requires a knowledge of κ and the initial conditions of the system, $\theta_{vib}(0)$ and $\theta_{ph}(0)$. The energy transfer parameter at ambient pressures, $\kappa(V_0)$, can be computed from the experimental low temperature lifetime of the doorway mode, while the volume dependence of κ can be calculated, as shown below, from tabulated atom-atom potentials for the molecular solid, and its mode Grüneisen parameters, γ_i. Initially the vibrations are equilibrated at ambient temperature, so that $\theta_{vib}(0) = 300$ K for these calculations. The initial phonon quasitemperature of the shocked solid, $\theta_{ph}(0)$, can be calculated with a knowledge of the molecular solid's shock equation of state; i.e., the shock Hugoniot, Grüneisen parameter, Γ, and constant volume heat capacity, $C_V(T)$.

(B) Pressure-Dependent Multiphonon Up-Pumping. The specific volume dependent energy transfer parameter $\kappa(V)$ characterizes the rate of energy transfer to the doorway mode from the external modes. It can be calculated by obtaining the value at ambient pressure, $\kappa(V_0)$, as well as a volume dependent $\kappa(V_1)/\kappa(V_0)$. The value of $\kappa(V_0)$ can be calculated knowing $\tau(0)$, the lifetime of the doorway mode at low temperature:[5]

$$\kappa(V_0) = j\hbar\Omega/\tau(0)\Theta_e \quad (4)$$

where j is the number or degeneracy of doorway modes. In this equation, Θ_e is the equivalence temperature, the temperature at which the rate of up-pumping into the doorway mode is equal to the low temperature rate of relaxation of the doorway mode by two phonon emission. The parameter κ is related to $k_{2ph\rightarrow vib}$ in eq 2 through $\tau(0)^{-1} = (36\pi^2/\hbar)\langle V^{(3)}(V)\rangle\rho^{(2)}$. Equation 4 is important in that it allows one to use the experimental value for $\tau(0)$ to obtain the necessary information without actual knowledge of either the anharmonic coupling matrix element or the two phonon density of states. For naphthalene, up-pumping is dominated by a single doorway mode at $\sim$200 cm^{-1},[48] for which $\tau(0) = 3$ ps and $\Theta_e = 300$ K.[5,56] Then eq 4 gives $\kappa(V_0) = 2.7$ J mol^{-1} K^{-1} ps^{-1}.

The rate constant for multiphonon up-pumping at ambient pressure, $\kappa(V_0)$, is appropriate for describing a cold molecule suddenly brought into contact with a hot phonon bath. However, behind a shock front, pressure and density effects increase the rate of up-pumping into the doorway modes. The necessary rate constant for shock induced up-pumping $\kappa(V)$, can be determined from $\kappa(V_0)$ and a calculation of the ratio $\kappa(V_1)/\kappa(V_0)$ using tabulated atom–atom potential functions, as shown below. This method is generally applicable to a wide range of molecular materials, including naphthalene and HMX, and it yields a simple analytical expression which makes it possible to determine how the up-pumping rate increases with pressure. Even in the absence of knowledge of $\kappa(V_0)$, this method provides useful information on the relative rate of the pressure dependence of multiphonon up-pumping.

The principal effect of density on $\kappa(V)$ is the increase in the anharmonic coupling $\langle V^{(3)}(V)\rangle$, but there are lesser effects due to the pressure-induced increase of the phonon and doorway mode frequencies and the phonon density of states, and the possibility of opening up new doorway mode channels. Consideration of these effects yield a scaling relation as a function of compression:[48]

$$\frac{\kappa(V_1)}{\kappa(V_0)} = \frac{|\langle V^{(3)}(V_1)\rangle|^2}{|\langle V^{(3)}(V_0)\rangle|^2}\frac{|\rho_{ph}(\omega,V_1)|^2}{|\rho_{ph}(\omega,V_0)|^2}\frac{\Omega_{max}(V_1)}{\Omega_{max}(V_0)} \quad (5)$$

The three terms in eq 5 represent the effects of density on the anharmonic coupling, the phonon density of states, and the number of doorway modes.[48]

The anharmonic coupling $\langle V^{(3)}(V)\rangle$ increases with compression due to the decrease in intermolecular separation. For molecular crystals, the intermolecular potential, that is the interaction between pairs of nonbonded atoms, is well approximated as a sum of terms of the form

$$V(R) = A\exp(-BR) - CR^{-6} \quad (6)$$

where R is the interatomic separation, and A, B, and C are constants characteristic of the type of atom pair.[35] A similar model potential has been used to calculate the magnitudes of various anharmonic coupling matrix elements for crystalline naphthalene and benzene.[53,54] These are complicated calculations that are quite dependent on the specific details of the potential used. In this work, we use a simpler method in order to estimate the ratio, $\langle V^{(3)}(V_1)\rangle/\langle V^{(3)}(V_0)\rangle$. It will be seen that this estimate is not very dependent on the details of the potential, and is widely

applicable to molecular materials such as the explosives considered in this study.

Using eq 6 and recalling that $(\partial V(R)/\partial R)|_{R=R_0} = 0$, where R_0 is the equilibrium interatomic distance, the cubic anharmonic coupling averaged over many atom–atom pairs can be written as[48]

$$\left.\frac{\partial^3 V(R)}{\partial R^3}\right|_{R=R_0}(R-R_0)^3 = \frac{6C}{R_0^7}\left(\frac{56}{R_0^2}-B^2\right)(R-R_0)^3 \quad (7)$$

Compression of the solid alters the interatomic potentials felt by the atom pairs. The interatomic distances are decreased and the atom pairs oscillate about a new energy minimum located up the hard repulsive wall of the original potential. The interatomic potential for the compressed solid must be known to determine the change in the anharmonic coupling. This potential is determined by assuming it has the same canonical form as the equilibrium solid, given by eq 6. The details of the shape of the potential in the compressed solid cannot be determined from the potential before compression, so it is assumed that the hard, repulsive part, characterized by the parameters A and B, is not effected by small amounts of compression. Given this ansatz, the new potential is unique, since the change in the equilibrium distance under compression, ΔR_0, determines the value of the sole remaining parameter C, characterizing the soft attractive part. For simplicity, we assume that ΔR_0 is given by

$$\Delta R_0 \equiv 1 - \frac{R_0(V_1)}{R_0(V_0)} \approx 1 - \left(\frac{V_1}{V_0}\right)^{1/3} \quad (8)$$

where $R_0(V_0)$ and $R_0(V_1)$ are the equilibrium interatomic distances in the uncompressed and compressed solids. Then an expression for the relative increase in cubic anharmonic coupling can be written using eq 7:

$$\frac{\langle V^{(3)}(V_1)\rangle}{\langle V^{(3)}(V_0)\rangle} = (1-\Delta R_0)\exp[BR_0(V_0)\Delta R_0]\left[1+\frac{B^2R_0^2(V_0)\Delta R_0}{56-B^2R_0^2(V_0)}\right] \quad (9)$$

Here B is the exponential parameter for the uncompressed solid.

Equation 9 shows that the relative increase in $\langle V^{(3)}\rangle$ is determined by the shape of the steeply rising repulsive wall, characterized by B, and is independent of the depth or width of the well. To model naphthalene and most common secondary explosives including the nitramines, only ten types of atom–atom interaction atoms need to be considered, those between C, H, N, and O atoms. The repulsive part of the potential for all 10 types of interactions is quite similar and is well approximated by $BR_0 = 13$.[35,57] Then eq 9 can be written in a particularly simple form, which does not depend on the details of the interatomic potential, and which can be applied to all materials consisting of C, H, N, and O atoms:

$$\frac{\langle V^{(3)}(V_1)\rangle}{\langle V^{(3)}(V_0)\rangle} \approx (1-\Delta R_0)\exp(13\Delta R_0)\left(1-\frac{3}{2}\Delta R_0\right) \quad (10)$$

Compression of a solid induces frequency shifts in the both phonon and vibrational modes. The volume dependence of the phonon and vibrational mode frequencies is described by mode Grüneisen parameters

$$\gamma_i = \partial \ln \omega_i / \partial \ln V \quad (11)$$

where ω_i is the mode frequency. In general, γ_i for phonon modes are much greater than γ_i for vibrational modes. Mode Grüneisen coefficients γ_i for naphthalene, measured by pressure-dependent Raman spectroscopy,[58,59] range from 2 to 5 for the phonons, whereas γ_i for naphthalene vibrational modes are typically 10^{-2}. The thermodynamic bulk Grüneisen parameter, $\Gamma = V(\partial p/\partial E)_V$, is the average of the mode-Grüneisen coefficients γ_i, weighted by the contribution of the mode to the specific heat $(C_V)_i$:[51,60]

$$\Gamma = \sum_i \gamma_i (C_V)_i \Big/ \sum_i (C_V)_i \quad (12)$$

Since the vibrational contribution to the bulk value is minimal, the average of the phonon mode Grüneisen parameters is quite close to the thermodynamic value of the bulk Grüneisen parameter. Therefore, Γ will accurately describe the overall frequency shifts of the acoustic and optical phonons in a compressed solid. For naphthalene the bulk Grüneisen parameter is 4.3.[35] For the following results, Γ was taken as directly proportional to the specific volume, so that $\Gamma/V \equiv G$ is a constant.[61,62]

The second and third terms in eq 5 account for pressure induced frequency shifts in the compressed solid. The second term in eq 5 accounts for compression effects on the phonon density of states. Compressing the material increases the number of phonons per unit volume, but increasing Ω_{max} reduces the number of phonons per unit frequency interval, so $\rho_{ph}(\omega,V)$ is linearly proportional to the material density and inversely proportional to Ω_{max}. The third term accounts for compression effects on the number of doorway modes. When the solid is compressed, Ω_{max} increases, but the doorway modes do not shift much. Doorway modes of large molecules lie in the range $\Omega_{max} \le \Omega \le 2\Omega_{max}$, so increasing Ω_{max} increases the width of this range, and the number of vibrations which fall into this range. So in large molecules with many vibrations, the number of doorway modes is roughly proportional to Ω_{max}. The density-induced frequency increase in Ω_{max} is calculated by integrating eq 11:

$$\frac{\Omega_{max}(V_1)}{\Omega_{max}(V_0)} = \exp\left(-\int_{V_0}^{V_1}\frac{\Gamma}{V}dV\right) \approx \exp(\Gamma_0\Delta V) \quad (13)$$

where the shock compression ΔV is given by

$$\Delta V = 1 - (V_1/V_0) \quad (14)$$

Then, the specific volume-dependent energy transfer parameter $\kappa(V)$ is given by eq 5 as

$$\kappa(V) = \kappa(V_0)\left|\frac{\langle V^{(3)}(V_1)\rangle}{\langle V^{(3)}(V_0)\rangle}\right|^2 (1-\Delta V)^{-2}\exp(-\Gamma_0\Delta V) \quad (15)$$

where $\kappa(V_0)$ is given by eq 4, the cubic anharmonic coupling term is given by eq 10, and Γ_0 is the bulk Grüneisen parameter at ambient pressure.

In Figure 3a, we show how $\langle V^{(3)}\rangle$ increases with compression by plotting $\langle V^{(3)}(V_1)\rangle/\langle V^{(3)}(V_0)\rangle$ as a function of the compression ratio V_1/V_0, for C–C, C–H, and H–H nonbonded atom–atom interactions. The values of B in eq 6 used for this calculation were obtained by fitting the naphthalene crystal structure and phonon dispersion curves obtained from neutron scattering.[53] The increase in $\langle V^{(3)}\rangle$ with compression is practically the same for C–C, C–H, and H–H interactions, with the exception of H–H which was marginally smaller. In fact, we find, using tabulated potentials for N and O interactions,[35] that the increase in $\langle V^{(3)}\rangle$ is nearly identical to those for C–C and C–H, demonstrating the accuracy of the approximation used to derive eq 11. Therefore it is possible to determine as a function of shock pressure the relative increase in the up-pumping rate parameter $\kappa(V_1)/\kappa(V_0)$, which is valid for most organic secondary explosives. The compression dependence of the up-pumping rate parameter $\kappa(V_1)/\kappa(V_0)$ is shown in Figure 3b. It is important to note that for most secondary explosives, κ increases by about a factor of 2 at 10 GPa.

(C) Initial Conditions for Up-Pumping Model. *(1) Shock Hugoniot.* The shock Hugoniot characterizes the irreversible process of shock compression. It is defined by the dual requirements of energy and momentum conservation across the

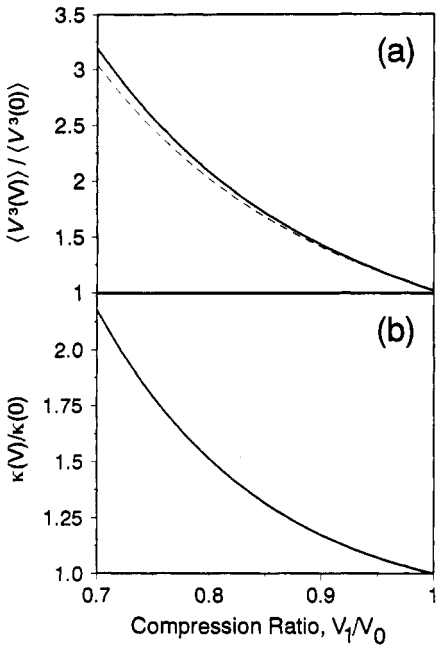

Figure 3. (a) Increase in cubic anharmonic coupling $\langle V^{(3)}(V)\rangle$ at specific volume V, relative to the value at ambient pressure $\langle V^{(3)}(0)\rangle$, calculated using eq 8 for C–C and C–H atom pairs (solid curve) and H–H pairs (dashed curve). The coupling increase for different atom pairs is practically identical, because it depends almost entirely on the steep repulsive part of the potential. (b) Increase in the up-pumping rate parameter $\kappa(V)$ at specific volume V, relative to the value at ambient pressure $\kappa(V_0)$, computed using eq 15.

shock layer. By energy conservation, the energy deposited in the solid across the shock front is given by

$$\Delta E = E_1 - E_0 = \frac{1}{2}(p_1 + p_0)(V_0 - V_1) \tag{16}$$

where the initial pressure p_0 is taken as zero. Momentum conservation allows the compression ratio and pressure rise across the shock front to be written in terms of the velocity of the shock wave in the solid, U_s, and the mass or impact velocity used to generate the shock, U_p:[38]

$$V_1/V_0 = U_p/(U_s - U_p) \tag{17}$$

$$p_1 - p_0 = U_s U_p / V_0 \tag{18}$$

Hugoniot measurements are usually given in the form[12,38]

$$U_s = b + mU_p \tag{19}$$

where m and b are empirical parameters. Other properties of the shock follow from a knowledge of m and b. The shock velocity is related to the shock compression ΔV by

$$U_s = \frac{b}{1 - m\Delta V} \tag{20}$$

Both p and dp/dV are related to ΔV by

$$p = \frac{b^2 \Delta V}{V_0(m\Delta V - 1)^2} \tag{21a}$$

$$\frac{dp}{dV} = \frac{b^2(m\Delta V + 1)}{V_0^2(m\Delta V - 1)^3} \tag{21b}$$

Equation 21a can be used to determine the relationship between the shock pressure p_1 and the shock compression ratio V_1/V_0 for naphthalene as shown in Figure 4.

The Hugoniot data for anthracene used for this study[37,38] give the values $b = 3.225$ km/s and $m = 1.452$. The physical properties of HMX differ somewhat from naphthalene and anthracene,[29]

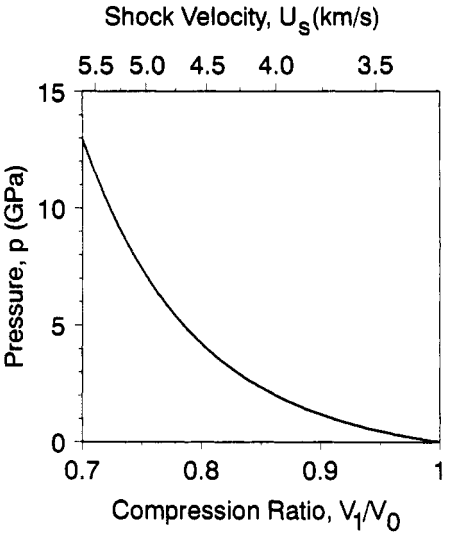

Figure 4. Shock Hugoniot measured for anthracene, giving the relation between the shock compression ratio V_1/V_0, the shock velocity U_s and the shock pressure p.

but nevertheless the Hugoniot for HMX, $b = 3.05$ km/s and $m = 1.705$,[38] gives practically identical results in the pressure regime of interest.

(2) Temperature Increase in the Shocked Solid. The shock-induced temperature increase in a solid can be calculated from the shock Hugoniot and the Grüneisen parameter, Γ. The first and second laws of thermodynamics are combined to yield

$$dS = \frac{C_V}{T}dT + \frac{\Gamma C_V}{V}dV \tag{22}$$

From eq 16, the differential change in internal energy, E, due to the shock is

$$dE = {}^1/_2(V_0 - V_1)\,dp - {}^1/_2 p\,dV \tag{23}$$

Substituting eq 23 into the thermodynamic relation $T\,dS = dE + p\,dV$ gives

$$T\,dS = \left[\frac{1}{2}(V_0 - V_1)\frac{dp}{dV} + \frac{1}{2}p\right]dV \equiv f(V)\,dV \tag{24}$$

where $f(V)$ is defined as the quantity in brackets above. Since the shock process is irreversible ($S \neq 0$), eqs 22 and 24 can be equated, which yields the differential expression[61]

$$\frac{dT}{dV} + GT = \frac{f(V)}{C_V(T)} \tag{25}$$

where $G = \Gamma/V$. Then for naphthalene, $G(V) = \Gamma_0/V_0 = 4.3/0.87 = 4.92$.[35] Equation 25 is solved for T_1 using an integrating factor, giving[61,63]

$$T_1 = T_0 e^{G(V_0 - V_1)} + e^{-GV_1}\int_{V_0}^{V_1} \frac{f(V)e^{GV}}{C_V(T)}dV \tag{26}$$

The first term in eq 26 is the temperature increase due to a reversible adiabatic compression, while the second term is the additional temperature increase due to the irreversible entropy increase along the Hugoniot.

The heat capacity $C_V(T)$ in eq 26 is calculated using the expression

$$C_V(T) = C_{V,ph} + C_{V,vib}(T) = 6k_B + k_B\sum_{i=1}^{n}\frac{\phi_i^2 \exp(-\phi_i/T)}{[1 - \exp(-\phi_i/T)]^2} \tag{27}$$

At temperatures of interest, the phonon constant volume heat capacity is independent of temperature, $C_{V,ph} = 6k_B$/molecule, since $\Omega_{max}/k_B T < 1$, where Ω_{max} is the phonon cutoff frequency.

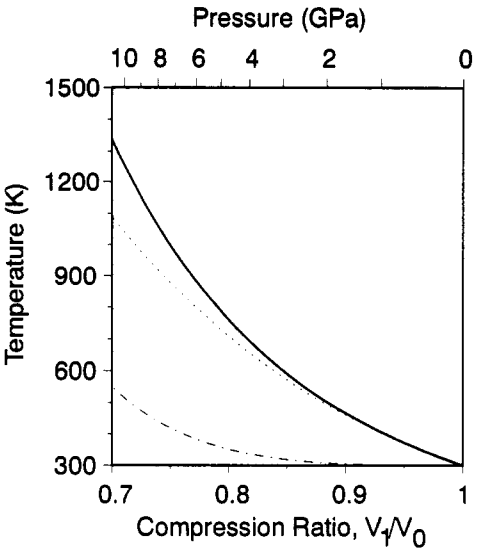

Figure 5. Final temperature T_1 of naphthalene irreversibly heated by a shock wave (solid curve). The shock-produced temperature increase can be separated into two parts (see eq 26), one being the temperature increase expected from reversible compression to the same final volume (dotted curve) and the remainder being the contribution from the irreversible part (dot–dashed curve).

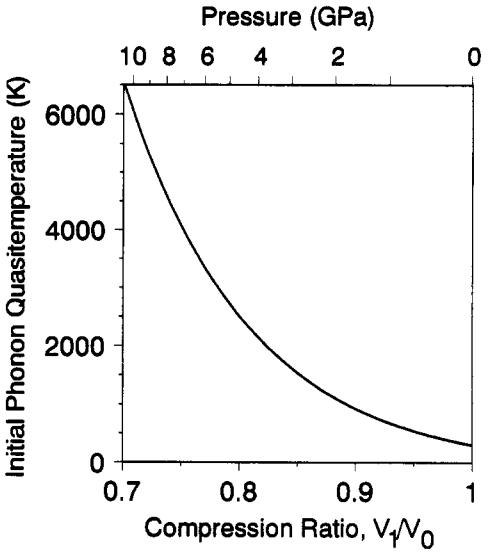

Figure 6. Initial phonon quasitemperatures, $\theta_{ph}(0)$, as a function of shock compression ratio calculated using eq 29.

For naphthalene, $\Omega_{max}/k_B \approx 200$ K.[35] The temperature dependence of the vibrational contribution to the heat capacity, $C_{V,vib}(T)$ cannot be neglected due to the quantum mechanical nature of the high frequency vibrations, so it is calculated using a sum of n independent Einstein oscillators with characteristic temperatures ϕ_i.[5] For naphthalene, $n = 48$ and the values of ϕ_i are tabulated.[49]

Figure 5 shows the shock-induced temperature rise for naphthalene, for shock pressures in the 0–10-GPa range, computed using eqs 26 and 27. For the relatively weak shocks considered, the contribution of the second (irreversible) heating term in eq 26 is less significant than the first (reversible) term, being less than 30% at the highest pressures considered. Figure 5 displays the final temperature, T_1, that is reached once an unreacted system has come to thermal equilibrium, i.e., all degrees of freedom are at the temperature T_1.

(3) Initial Phonon Quasitemperature. When the shock front passes through a region of the material, the shock excites phonons first.[1,3-5,14] This can be demonstrated using a thermodynamic argument. Equation 26 shows that the temperature rise is an exponentially increasing function of the Grüneisen coefficient. In fact, when expanded according to eq 12, the temperature jump across the shock front for each individual mode is an exponentially increasing function of γ_i. So the initial increase in phonon quasitemperature is far greater than the increase in vibrational quasitemperature.

The specific distribution of excited phonons produced near the shock front could, in principle, be computed knowing the direction of shock propagation and the mode Grüneisen *tensor*, but it is also important to consider the likelihood of energy redistribution *among the phonons*, which drives any initial distribution of shock-excited phonons toward a quasi-thermal distribution. It is known that the large anharmonic coupling characteristic of phonon states in molecules crystals leads to rapid phonon–phonon scattering occurring on the one ps time scale, about what is required for the passage of the shock front through a few molecular planes.[3,14,48,64] The efficiency of these redistribution processes allows the initial state of the phonon bath behind the front to be accurately characterized by the initial phonon quasitemperature, $\theta_{ph}(0)$.

The initial phonon quasitemperature $\theta_{ph}(0)$ is obtained using the fact that essentially all heat, ΔH, added by the shock to the solid is initially deposited into the phonons and quickly redistributed into a state of quasiequilibrium among the phonons.[3] Then, for a shock compression resulting in a final equilibrium temperature T_1, the heat added to the phonons is

$$\Delta H_{ph} = \Delta H = \int_{T_0}^{T_1} C_p(T)\,dT \tag{28}$$

The initial phonon quasitemperature can then be calculated by

$$\theta_{ph}(0) = T_0 + \int_{T_0}^{T_1} \frac{C_p(T)}{C_{p,ph}}\,dT = T_0 + \int_{T_0}^{T_1} \frac{C_V(T)}{C_{V,ph}}\,dT \tag{29}$$

where the latter equality follows from the thermodynamic relationship

$$C_p(T) = C_v(T)(1 + \Gamma\alpha T) \tag{30}$$

Here α is the coefficient of thermal expansion and Γ is the Grüneisen parameter.

Figure 6 displays the initial phonon quasitemperature as a function of shock compression and pressure. The initial phonon quasitemperature is always much greater than T_1. In naphthalene between 300 and 1200 K, the phonon heat capacity $C_{V,ph}$ ranges from $^1/_3$ to $^1/_5$ of the total heat capacity, C_V. So $\theta_{ph}(0)$ will be 3–5 times greater than T_1. This can be seen by comparing Figures 5 and 6.

(D) Time Dependence of Multiphonon Up-Pumping in the Bulk Material. With the pressure dependence of the cubic anharmonic coupling, $\langle V^{(3)} \rangle$, and the up-pumping rate parameter, κ, it is possible to determine how the rate of up-pumping is affected by compression of the medium and to calculate the time dependence of the up-pumping explicitly, using eqs 3.[5] The first equation describes the fall of the phonon quasitemperature as energy flows from the phonon bath into the vibrations. The second equation describes the rise in the vibrational quasitemperature. The time dependencies of the two quasitemperatures in eqs 3 were calculated by numerical integration, using a Runge–Kutta algorithm. A chosen value of the shock pressure p, or shock compression ratio V_1/V_0 determines the final thermodynamic temperature T_1 (Figure 5), the initial phonon quasitemperature $\theta_{ph}(0)$ (Figure 6), and the ratio $\kappa(V_1)/\kappa(V_0)$ (Figure 3). For naphthalene,[5] $\kappa(V_0) = 2.7$ J mol^{-1} K^{-1} ps^{-1}. Because insufficient data on the volume expansion coefficient $\alpha(p,T)$ over a wide range of T and p were available, we used the constant-volume heat capacity C_V from eq 27 rather than C_p from eq 30. Based on model calculations using $\alpha(p=0,T)$, we estimate this simplification produces no more than a 10% decrease in the rate of up-pumping.

The results of calculations for shock compression of naphthalene using eqs 3 are shown in Figure 7. The compression ratio is $V_1/V_0 = 0.80$, corresponding to a shock pressure of 4.7 GPa. In Figure 7, the phonons cool down from an initial state $\theta_{ph}(0) \approx$

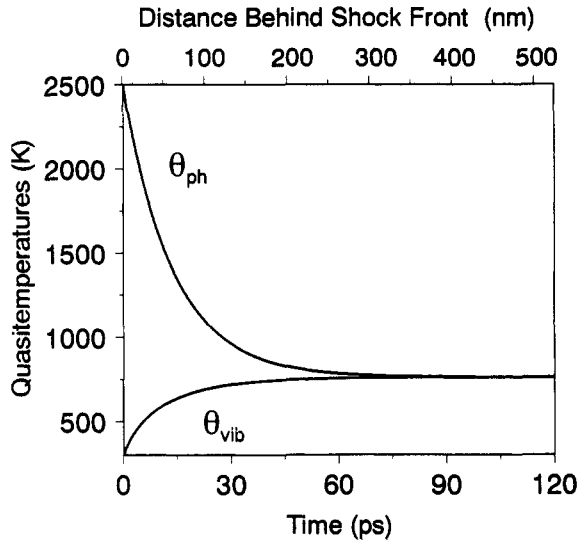

Figure 7. Time dependence of the phonon quasitemperature, θ_{ph}, and the vibrational quasitemperature, θ_{vib}, for a shock compression ratio $V_1/V_0 = 0.80$ ($p = 4.7$ GPa). Multiphonon up-pumping transfers energy from the hot phonon bath to internal molecular vibrations. Because the vibrational contribution to the heat capacity is much larger than the phonon contribution, θ_{ph} drops much farther than θ_{vib} rises. Most of the vibrational up-pumping is complete in 30 ps, and the system has reached thermal equilibrium in ~70 ps.

2500 K to a final state $\theta_{ph} = T_1 \approx 760$ K. The vibrations heat up from an initial state $\theta_{vib}(0) = T_0 = 300$ K to a final state $\theta_{vib} = T_1 \approx 760$ K. One of the important features of this model is the significant disparity in cooling rates. The rate constant for phonon cooling, κ/C_{ph} is much larger than the rate constant for vibrational heating, κ/C_{vib} because $C_{vib} \gg C_{ph}$. The figure shows that the time scale for multiphonon up-pumping is a few tens of ps. Most of the rapid rise in vibrational quasitemperature is complete by 30 ps, and the system has reached the thermal equilibrium temperature, T_1, by approximately 70 ps. Figure 8 displays the time dependence of the phonon quasitemperature cooling and the vibrational quasitemperature heating for several values of the compression ratio. A smaller compression ratio (stronger shock) results in a higher initial phonon quasitemperature and a higher final vibrational temperature. However, independent of the strength of the shock, most of the rise of the vibrational quasitemperature occurs in 30 ps, and thermal equilibrium is reached in approximately twice this time. The details of the time dependencies calculated here depend on the naphthalene parameters used in the calculations. However, for molecular solids as large or larger than naphthalene which have similar Γ, $\tau(0)$, and C_V parameter, such as HMX, the results should not vary by more than a factor of two from those presented in Figures 7 and 8.

Calculations like those shown in Figure 8 can be used to determine the up-pumping time, t_{up}, and the width of the up-pumping zone, l_{up}. We define t_{up} and l_{up} as the time and distance from the shock front, $\theta_{ph} = \theta_{ph}(0)$, to the 90% point, where $\theta_{ph} = 0.1(\theta_{ph}(0) - T_1) + T_0$. For all shock compression ratios ($0.70 < V_1/V_0 < 1.0$), t_{up} is nearly constant at 30 ps. Smaller compression ratios (stronger shocks) result in higher up-pumping rate, but the vibrational temperature rise to reach T_1 is also greater. These two factors effectively negate each other.

Since t_{up} is a nearly constant function of compression, the width of the up-pumping zone l_{up}, shown in Figure 9, reflects the increase in the shock velocity for smaller compression ratios as given by the Hugoniot. The plot reflects the slight variations in t_{up}, combined with the rise in shock velocity with compression ratio. The nonzero value at $V_1/V_0 = 1.0$ reflects the phonon relaxation time for small, linear perturbations, that relax at approximately the speed of sound.

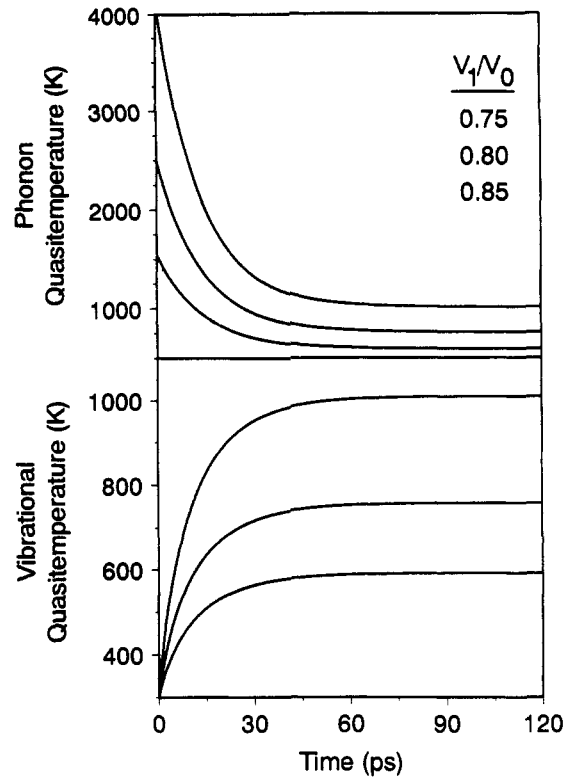

Figure 8. Fall in phonon quasitemperatures (top) and the corresponding rise in vibrational quasitemperatures (bottom) due to vibrational up-pumping for several compression ratios. The compression ratios correspond directly to the curves in both top and bottom. Note the difference in temperature scales on top and bottom. In all cases, most of the vibrational up-pumping occurs in 30 ps and thermal equilibrium is reached in ~70 ps.

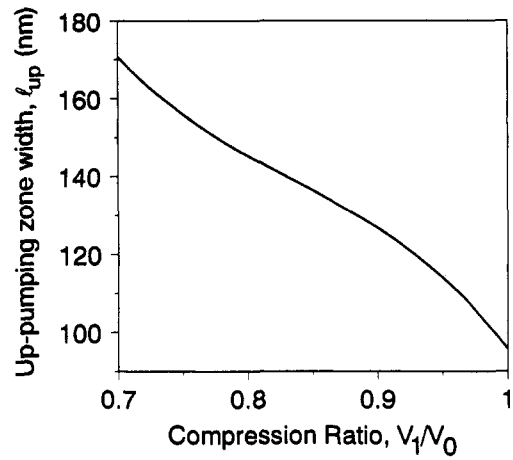

Figure 9. Width of the up-pumping zone for various values of the shock compression ratio. The form of the plot arises from slight variations in t_{up}, combined with the rise in shock velocity with compression ratio.

III. Multiphonon Up-Pumping in Defect Perturbed Domains

Here we will be concerned with defect perturbed domains (DPD) in which the anharmonic coupling of the phonon bath to the doorway modes is greater than in the bulk. It is shown below that this causes the DPD vibrational quasitemperature θ_d to overshoot the maximum temperature in the bulk. On a short time scale, the molecular vibrations in DPDs are pumped faster and higher than the bulk, resulting in hot spots. The DPD anharmonic coupling matrix element can be described by[5]

$$\langle V^{(3)}(V)\rangle_{DPD} = \xi\langle V^{(3)}(V)\rangle_{bulk} \qquad (31)$$

where $\xi > 1$ is the defect enhancement factor. The defect enhancement factor can also be a function of compression, but for the sake of simplicity we have assumed the volume dependence

of anharmonic coupling is the same in the DPD and in the bulk.

There are many different kinds of defects which could produce perturbed domains with enhanced anharmonic coupling. For example, a defect might consist of an impurity molecule with a larger dipole moment, or a larger size, that produces a strain dipole.[65] In both cases, the perturbation of the surroundings falls off quite slowly, as R^{-3}. The packing of the bulk molecules around an impurity can enhance the anharmonic coupling, due to the accommodation of the structurally incompatible molecule. This perturbation extends over long distances. The defect also lowers the symmetry of the DPD. This opens up new channels for the up-pumping, which, in the absence of a defect, are forbidden in the higher symmetry perfect crystal space group. Thus a DPD can potentially give rise to a hot spot of significant volume.[31,32]

Two examples of energy transfer in DPDs which are much larger than the impurity molecules themselves are found in works by Wilson et al.[31] and by Walker.[4] Using time-resolved coherent Raman scattering, naphthalene phonon lifetimes perturbed by the presence of pentacene impurities were studied.[31] Impurity-perturbed domains dominated the bulk material at a pentacene concentration of $\sim 10^{-5}$ mol/mol, which implies that a single pentacene impurity can perturb 10^5 bulk molecules. It was shown that for optical phonons in the impurity-perturbed domains, lifetimes were reduced by a factor of four, corresponding to $\xi \approx 2$ in eq 31. This measurement shows that the enhancement of the anharmonic coupling between optical phonons and acoustic phonons can be at least a factor of two. So the anharmonic coupling between optical phonons and doorway modes, which is relevant to up-pumping, should be enhanced by a factor of the same magnitude. Detonation studies[4] showed that 0.05% of diethylenetriamine can substantially decrease the time to initiation and detonation velocity of nitromethane, suggesting that each impurity can perturb 2000 bulk molecules. The defect anharmonic enhancement mechanism does not require the presence of extrinsic impurities in the energetic material. Even perfect, single crystals can be perturbed by intrinsic defects created in the wake of the passing shock front. So a shock can sow a stream of DPDs in its wake. These defects might be molecular fragments produced by the large strain gradients at the front,[4,36,66] or phase separated domains produced by pressure-induced phase transitions like the β to δ-HMX transition.[67]

In the DPD, the rate of vibrational up-pumping is proportional to $\xi^2\kappa$. In a manner analogous to eqs 3, the shock pumping of the bulk and defect vibrations can be described by[5]

$$\frac{\partial \theta_{ph}}{\partial t} = \frac{\kappa(V)(1-\chi_d)}{C_{p,ph}}[\theta_{vib} - \theta_{ph}] + \frac{\xi^2\kappa(V)\chi_d}{C_{p,ph}}[\theta_d - \theta_{ph}] \quad (32a)$$

$$\frac{\partial \theta_{vib}}{\partial t} = \frac{\kappa(V)}{C_{p,vib}(\theta_{vib})}[\theta_{ph} - \theta_{vib}] \quad (32b)$$

$$\frac{\partial \theta_d}{\partial t} = \frac{\xi^2\kappa(V)}{C_{p,vib}(\theta_{vib})}[\theta_{ph} - \theta_d] \quad (32c)$$

In eqs 32, χ_d is the DPD fraction of the solid (the fraction of molecules perturbed by defects), and we have assumed for simplicity that the intensive heat capacity of the DPD vibrations is identical to that of the bulk. In addition to the factors contained in eqs 3 for bulk up-pumping, the DPD vibrational quasitemperature depends on the χ_d and the anharmonic enhancement, ξ. Here we consider small DPDs ($\chi_d \ll 1$), since large DPDs were discussed previously.[5]

In a DPD characterized by $\xi > 1$, the vibrations are pumped by the phonons faster than the bulk vibrations, so the DPD vibrational quasitemperature, θ_d, will overshoot the bulk vibrational quasitemperature θ_{vib}. In fact, as eqs 32 demonstrate, with extremely large values of ξ, the time dependent behavior of θ_d approaches $\theta_{ph}(0)$, which can be 3–5 times as large T_1, the maximum bulk vibrational quasitemperature. A large vibrational quasitemperature difference, $\theta_d - \theta_{vib}$, which is actually a spatial gradient of excitation, can exist in the solid because of energy transfer from the hot defect vibrations to the colder bulk vibrations. Direct vibration-to-vibration energy transfer is quite inefficient in molecular crystals, since molecular vibrations are practically localized on individual molecules.[5,48,49] This is in contrast to delocalized phonons. A sizable spatial gradient of phonons will equilibrate very rapidly. The rapid phonon equilibration will maintain the DPD phonon quasitemperature at the bulk value although θ_d exceeds θ_{vib}.

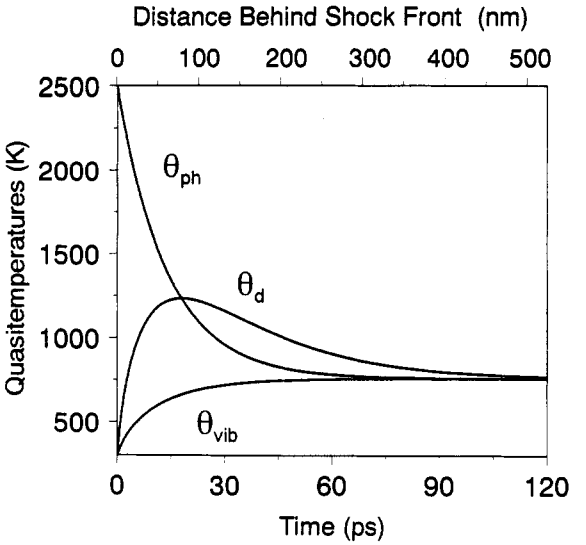

Figure 10. Time dependence of the phonon quasitemperature, θ_{ph}, the bulk vibrational quasitemperature, θ_{vib}, and the defect perturbed domain vibrational quasitemperature, θ_d, for a shock compression ratio $V_1/V_0 = 0.80$ ($p = 4.7$ GPa) and a DPD anharmonic enhancement $\xi = 2$. The greater anharmonic coupling in the DPD causes its vibrations to come into equilibrium with the hot phonons faster than the bulk vibrations, producing a temporary temperature overshoot and a transient hot spot.

Two factors determine the peak DPD vibrational quasitemperature: the shock compression ratio V_1/V_0, and the defect enhancement factor ξ. A typical calculation of the three quasitemperatures is shown in Figure 10 for $V_1/V_0 = 0.8$ ($p = 4.7$ GPa), and $\xi = 2.0$. θ_{ph} and θ_{vib} are the same as in Figure 7. θ_d rises faster and peaks at a much higher temperature than θ_{vib}. Therefore, a transient hot spot is created in the DPD due to enhanced anharmonic coupling. Because DPD vibrations equilibrate with the phonons so rapidly, hot spots are formed right behind the shock front, typically within 50 nm of the front. Phonons and bulk vibrations equilibrate in about 70 ps, while the hot spot, which heats up *and* cools down, equilibrates with the bulk in about 120 ps. If the hot spot reacts, it will generate additional heat and will not cool down as shown in Figure 10. Just after the shock front passes, the molecules in the DPD absorb phonons faster than the bulk. If the χ_d is small, which is the case being considered here, it does not deplete the phonon bath, and therefore has little effect on the up-pumping of the bulk material. But if χ_d is large, as when the DPD is present in a small isolated grain of material, there will not be enough excited phonons in the grain to produce the large temperature overshoot needed for ignition. This suggests a size effect in hot spot initiated shock chemistry.[5] The prediction, that small grains should be less reactive than large grains, has been observed in some experiments.[68,69] It is important to distinguish the size effect on reactivity predicted by our model from the size effect observed in detonation studies. Detonation properties are not a simple function of grain size since grain size changes the reaction probability as well as the porosity, which has a significant effect on the likelihood of detonation.[69]

Figure 11 displays the DPD vibrational quasitemperature for varying values of ξ for $V_1/V_0 = 0.80$. The dashed curve is the bulk vibrational quasitemperature, and the solid curves show the

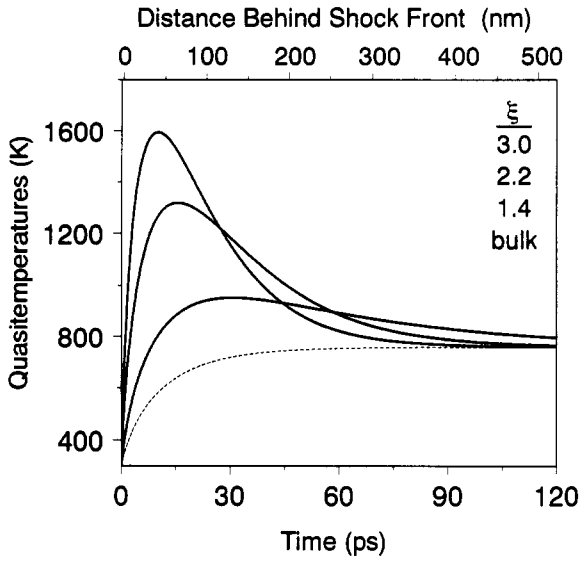

Figure 11. Defect vibrational quasitemperatures for shock compression $V_1/V_0 = 0.80$ ($p = 4.7$ GPa) for various values of the anharmonic enhancement ξ, compared to the bulk ($\xi = 1$) vibrational quasitemperature (dashed curve). For larger values of ξ, the defect comes into equilibrium with the hot phonons faster. The peak defect temperature increases with ξ, and the hot spot reaches its peak temperature a short distance, typically 50–100 nm, behind the front. It can be seen that even a very modest anharmonic enhancement of 1.4 can result in a substantial increase in the maximum vibrational temperature.

results for three values of ξ. The peak θ_d, which clearly depends greatly on ξ, is important because it determines the extent of bond-dissociation reactions and, together with the DPD size, whether the DPD can ignite the surrounding material.

IV. Reaction Probability in Bulk and in Defect Perturbed Domains

Behind the up-pumping zone (~30 ps), chemical reactions can be described using Arrhenius kinetics. But within this zone, a bulk temperature does not exist, so ordinary Arrhenius expressions must be modified by using the vibrational quasitemperature in place of T. Molecules in this zone at constant pressure p_i are subjected to a sudden increase in this quasitemperature characterized by the function $\theta_{vib}(t)$. It is therefore necessary to calculate the probability of a molecule undergoing a reaction in time t, $N(p,t)$ for a time dependent $\theta_{vib}(t)$.

For the unimolecular thermal decomposition reactions considered here, transition-state theory gives the rate constant $k(p,T)$ as

$$k(p,T) = \frac{k_B T}{h} \exp[\Delta S^*(p)/R] \exp[-\Delta H^*(p)/RT] \quad (33)$$

where $\Delta S^*(p)$ is the pressure-dependent activation entropy and $\Delta H^*(p)$ is the pressure-dependent enthalpy of activation. HMX solid-state unimolecular thermal decomposition has been studied at ambient pressure[39,70] and between 3.6 and 6.5 GPa.[40] However, the latter measurements were obtained over a narrow range of temperature (553–568 K). To find a consistent form for $k(p,T)$ which is reasonably accurate over a wide range of p and T (T will be replace by $\theta_{vib}(t)$), we chose a form for $k(p,T)$ which gives the correct value as $p \to 0$, and which has the correct pressure dependence. Increasing the pressure *slows down* thermal decomposition reactions because $\Delta V^* > 0$, where ΔV^* is the activation volume. For HMX, $\Delta V^* = 4.1$ cm^3/mol, and is approximately independent of pressure.[40]

The pressure dependence of ΔS^* and ΔH^* can be modeled with the linearized relations:

$$\Delta S^*(p) = \Delta S^*(0) + p(\partial \Delta S^*/\partial p)_{p=0} \quad (34a)$$

$$\Delta H^*(p) = \Delta H^*(0) + p(\partial \Delta H^*/\partial p)_{p=0} \quad (34b)$$

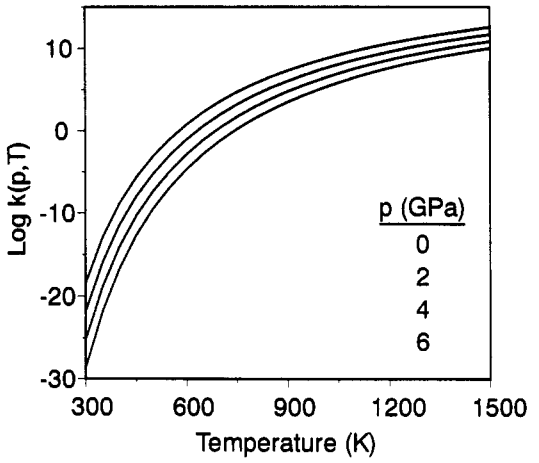

Figure 12. Chemical reaction rate constants for HMX thermal decomposition, $k(p,T)$, versus temperature for various values of pressure. Increasing the pressure decreases the rate constant because the activation volume $\Delta V^* > 0$.

The initial values $\Delta S^*(0) = 128$ J/mol K and $\Delta H^*(0) = 218$ kJ/mol, were determined using $p = 0$ thermal decomposition data.[39,70] The derivatives in eqs 34, which describe the pressure dependent change in ΔS^* and ΔH^*, can be calculated from the thermodynamic identities:

$$\left(\frac{\partial \Delta S^*}{\partial p}\right)_T = -\left(\frac{\partial \Delta V^*}{\partial T}\right)_p = -\alpha^* \Delta V^* \quad (35a)$$

$$\left(\frac{\partial \Delta H^*}{\partial p}\right)_T = T\left(\frac{\partial \Delta V^*}{\partial T}\right)_p + \Delta V^* = \Delta V^*(\alpha^* T + 1) \quad (35b)$$

where $\alpha^* = (\Delta V^*)^{-1}(\partial \Delta V^*/\partial T)_p$ is the thermal expansion coefficient of the activated complex, assumed to be identical to the bulk expansion coefficient. Then we find $(\partial \Delta S^*/\partial p)_T = -2$ J/(mol K GPa) and $(\partial \Delta H^*/\partial p)_T = 5$ kJ/(mol GPa) for HMX. With these parameters, eqs 33 and 34 can be used to compute $k(p,T)$ over the p, T range of interest, as shown in Figure 12. Then, knowing $k(p,T)$, the reaction probability is

$$N(p,t) = 1 - \exp\left[-\int_0^t \frac{k_B \theta(t')}{h} \exp[\Delta S^*(p)/R] \times \exp[-\Delta H^*(p)/R\theta(t')]\, dt'\right] \quad (36)$$

where $N(p,0) = 0$. In eq 36, $\theta(t)$ refers to either the DPD or bulk vibrational quasitemperature profile as calculated by eqs 32.

For a given set of vibrational quasitemperature profiles, as in Figure 10, the reaction probability $N(p,t)$ is calculated by numerical integration of eq 36, for bulk molecules or DPD molecules, using $\theta_{vib}(t)$ or $\theta_d(t)$, respectively. Figure 13 shows results for the bulk material ($\xi = 1$) and for DPDs with anharmonic enhancement ($\xi > 1$). The different panels are for various compression ratios. It is evident from Figure 13 that a small increase of ξ above unity enhances the defect reaction probability by many orders of magnitude relative to the bulk. For example, at $V_1/V_0 = 0.80$ (Figure 13a) and $\xi = 2$, the probability of a reaction in the DPD exceeds that in the bulk by about 10^8. For $V_1/V_0 = 0.85$ (Figure 13b) at 40 ps, the bulk reaction probability is $\sim 10^{-9}$ while for $\xi = 2$, the DPD reaction probability is $\sim 10^{-1}$. At high compression, the enhancement of DPD reactivity is unimportant since both the bulk and the DPD react completely. The DPD reaches a reaction probability of unity faster than the bulk and closer to the shock front, but since the bulk also obtains unit reaction probability, the few tens of ps difference in time will be insignificant. The net result is that the anharmonic enhancement of DPD reactivity takes on the greatest significance for relatively weak shocks.

The reaction probability for the bulk begins to approach unity for $V_1/V_0 \approx 0.70$, as shown in Figure 13d. This model predicts

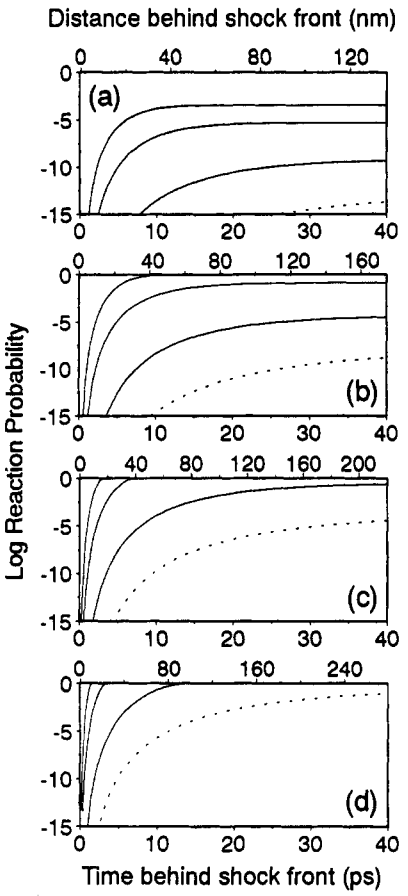

Figure 13. Computed time dependent chemical reaction probabilities for defect perturbed domains and bulk material for shock compression values of (a) 0.85, (b) 0.80, (c) 0.75, and (d) 0.70. In each panel, solid lines refer to anharmonic enhancements ξ of 2.6, 2.0, and 1.6, from top to bottom. The bulk reaction probability ($\xi = 1$), given by the dashed curves, remains small until the compression $V_1/V_0 \approx 0.70$.

that a shock of about 10 GPa should be sufficient to reproducibly initiate ideal, defect-free, crystalline HMX. Most available experimental data on HMX initiation involves studies of HMX formulations, such as PBX 9404,[22] rather than large single crystals. However, studies of single crystal HMX excited by an exploding foil shock driver, show complete bulk reaction under a shock pressure of 12.8 GPa, while those under a pressure of 7.0 GPa are nonreactive.[71] The results of these experiments are clearly in agreement with our prediction.

An important question is whether the ignition of the DPD will also cause the surrounding material to ignite. Elementary models like the Frank–Kaminetsky thermal explosion criterion[72] can be used to establish the likelihood of reaction spreading from a hot spot by balancing the rate of heat evolution by chemical reaction with the rate of heat loss by thermal conduction. In several studies, the likelihood of the reaction spreading from a hot spot was found to be a roughly linear relation between the reciprocal of the peak hot spot temperature and the log of the hot spot diameter.[30,34] In other words, the reaction will spread from small spots if they are very hot, while larger spots may be somewhat cooler. McGuire's calculations for spherical hot spots of HMX,[30] shown in Figure 14, were used to determine ignition criteria for our hot spot calculations. Figure 14 can be used to determine the minimum size of the hot spot required to ignite the surroundings for a particular value of V_1/V_0 and ξ. The dashed lines are for various hot spot diameters. The solid curves are for several compression ratios. For particular values of V_1/V_0 and ξ, if the point is above a dashed curve, then a DPD of size corresponding to the dashed curve will ignite the surrounding material. For example, given a DPD enhancement of $\xi = 2$, a 0.1-μm-diameter DPD will ignite the surroundings when $V_1/V_0 \leq 0.8$.

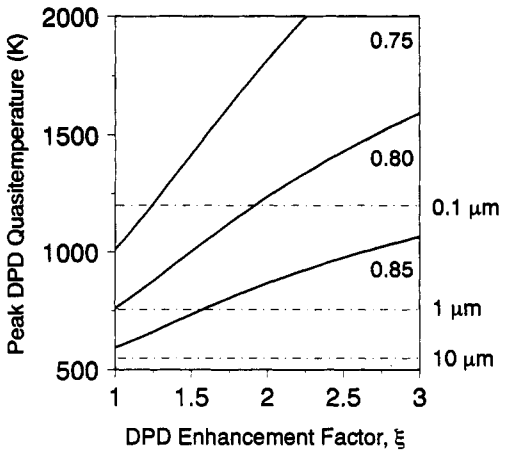

Figure 14. Peak defect perturbed domain vibrational quasitemperature for various values of shock compression and DPD anharmonic enhancement ξ. The probability that a reaction will spread from the DPD is approximately proportional to the log(DPD diameter) and the peak temperature. For a particular DPD diameter (dashed lines), the portion of the plane which lies above the dashed lines indicates a region where the reaction will spread from the DPD to the surroundings. For example, a 0.1-μm DPD with an enhancement factor of 2 experiencing a shock compression of 0.8 will ignite its surroundings.

V. Discussion

Detonation is a complex problem, in part due to the wide range of relevant time and length scales. For example, the shock front is a few nm wide, it crosses a line of molecules in 10^{-12} s, and up-pumping occurs on the 10^{-11} s time scale. In contrast, the Chapman-Jouguet plane is located perhaps 1 cm behind the front, and the characteristic time for equilibration of products in this plane is 10^{-8}–10^{-6} s.[19] Detonation pressures are enormous. For example, the detonation velocity and pressure of HMX is 10 km/s and 39 GPa, respectively.[73] Under these extreme conditions, hydrodynamic phenomena, not considered in the model, play an important role. Some of the hydrodynamic phenomena of interest include effects of immense shear forces at the front,[4] diffusion-controlled bimolecular reactions, plastic flow, dislocation pile ups,[1] and the layer-by-layer peeling off of molecules at the gas-to-solid interface.[74]

The model discussed here focuses on the propagation of a relatively weak shock through a nearly perfect solid. These are the conditions of greatest interest to designers of insensitive explosives. Insensitive explosives will be formulated in a manner designed to maximize density and minimize the amount of free volume, and most accidents which cause explosive detonations involve low-velocity impacts or fires which generate only compressive waves, stimuli which are rarely intense enough to directly initiate the materials.[7] In this case, conditions which favor the production of small hot spots are of the greatest importance, and these conditions are found in the highly nonequilibrium zones just behind the front.

In the past, proposed mechanisms for hot spot formation involved macroscopic hydrodynamic phenomena, and thus these mechanisms are of minimal importance in the case being considered. In our model, the mechanism of defect perturbed domains with anharmonic enhancement invokes strictly microscopic properties to form a macroscopic hot spot, and therefore hydrodynamics is no longer required. Instead the mechanism for hot spot formation involves the microscopic strain field or other perturbation in the vicinity of a small defect, which tends to concentrate the energy of the delocalized phonons produced in the wake of the shock front.

No thermochemical reaction can occur without some amount of vibrational activation. However, up-pumping takes on the greatest importance in the secondary explosive materials. Primary explosives are unstable molecules which have low reaction barriers, and the initial step is highly exothermic. As a consequence, these

materials are extremely sensitive, and only a small amount of multiphonon up-pumping is required to activate primary explosives. In shock-induced molecular activation, it is possible that primary explosives can react on the first hard collision. So one might expect the up-pumping zone in these materials to be extremely thin or absent altogether. That is what is observed in the molecular dynamics simulations of White et al.,[75] where the system considered has the characteristics of a primary explosive. The reaction barrier is quite low, ~600 cm^{-1}, whereas the vibrational frequencies are quite large, the lowest being ca. ~3000 cm^{-1}. As a consequence, reactions are observed immediately behind the front, and no up-pumping zone can be discerned.

Secondary explosives are quite stable molecules. A tremendous amount of energy must be transferred to the internal vibrations before any reaction occurs at all, and the first reaction steps to occur are endothermic. For HMX, the activation barrier is 215 kJ/mol,[39] or 18,000 cm^{-1}/molecule, which corresponds to the absorption of perhaps 180 phonons, whereas the lowest frequency molecular vibration is ca. 150 cm^{-1}. These molecules will not react on the first collision. The calculations show that significant amounts of multiphonon up-pumping require several tens of ps to occur. That corresponds to 10^2–10^3 collisions before the vibrations become chemically activated. So the up-pumping zone extends a finite distance behind the front. The calculations presented above indicate that this distance is ~100–170 nm. The necessity of pumping so much energy into these molecules before any is recovered explains the central importance of multiphonon up-pumping.

A result of the theoretical development presented here is a simple method of quantifying the pressure dependence of the various processes, which represents an important advance over the previous work.[5] Incorporation of pressure-dependent effects substantially improves the realism of the calculations. A great simplification was achieved by realizing that the effects of pressure on anharmonic coupling, a cubic derivative, are mainly controlled by the steep repulsive part of the potential.

In general terms, an increase in pressure results in (1) an increase in the shock wave velocity U_s and shock compression ΔV, (2) an increase in the number of phonons generated, characterized by $\theta_{ph}(0)$, (3) an increase in the up-pumping rate parameter κ, caused by increased anharmonic coupling and an increase in the number of doorway modes pumped, and (4) an increase in the barrier for the initial reaction step due to the positive activation volume characteristic of unimolecular decomposition reactions.

The quantitative results obtained in this model were based on data obtained for different molecules, however, they should be reasonably accurate. It was demonstrated that the increase of the cubic anharmonic coupling and the up-pumping rate on density was dependent only on the compression factor, and not the atomic composition, for most organic compounds. The heat capacity and Hugoniots of nitramine explosives and other organic molecules are reasonably similar,[38] and should not alter the quantitative results by more than a factor of two for similar molecules. The rate of up-pumping will be greatly affected by the number of doorway modes, their degeneracy, and their relaxation rate, as given by eq 4. Clearly, the up-pumping rate is dependent on the number of channels for up-pumping, so that a molecule with numerous low frequency vibrations acting as doorway modes will see greatly increased up-pumping. The Grüneisen parameter is the most critical variable in this model, as it effects both the magnitude of quasitemperatures and the up-pumping rate. It is hard to quantify the uncertainty in this parameter, as limited data is available. This would likely be the largest source of error in the up-pumping rate calculations. Further kinetic data, especially under high pressure, is needed to check and improve the accuracy of the reactivity results. The specific parameters used in this model are clearly quite reasonable, since they provide quantitative agreement with the measured value of shock pressure required to initiate HMX single crystals.[71]

Since there is a large amount of kinetic and thermodynamic data available on the reactions of the secondary explosives and their primary reaction products, it is also useful to assess the accuracy of Arrhenius kinetics in modeling reactions of secondary explosives. Arrhenius kinetics at the bulk temperature T_1 will be valid behind the up-pumping zone, which is typically 30 ps behind the shock front. Within the up-pumping zone, there is no temperature. Nevertheless it is possible to approximately characterize chemical rate process using Arrhenius-like expressions with the vibrational quasitemperature $\theta_{vib}(t)$ substituted for the thermodynamic temperature. This conclusion follows from the high efficiency of IVR processes in large molecules, which rapidly produces a nearly quasithermal distribution of vibrational excitation within the molecules.

This theoretical investigation suggests several directions for future research aimed toward a better understand of molecular energy processes behind the shock front. First, better data is needed on the doorway modes of important energetic materials, particularly at high pressures.[76] Time-resolved studies of relaxation processes of these molecules are highly desirable, and a new method for producing large temperature and moderate pressure jumps in molecular materials hold great promise.[16] Also high resolution far-infrared and Raman scattering studies would be sufficient to characterize the number of doorway modes and their low temperature relaxation rates. In particular, more needs to be learned about the dynamic behavior of amalgamated molecular vibrations in floppy molecules like nitramines. This information can be obtained by studying the frequency shift and broadening of vibrational transitions of isotopically mixed crystals.[77]

Another area of importance is studying how thermal decomposition kinetics are affected by the rate of heating. Currently, most experiments are performed at heating rates which are a dozen orders of magnitude smaller than the 10^{13} K/s heating characteristic of shock-wave processes. The experimental results often yield unrealistic results when used to describe sudden jumps to high temperatures, owing to preexponential factors of 10^{19} or larger.[39] Some of the interesting effects of ultrafast heating rates on solid-state decomposition have recently been studied using ultrafast optical calorimetry.[78]

Finally, the micromechanical nature of molecular defects, and the interaction of phonons with defect-perturbed domains[31] need further elucidation. Ultrafast nonlinear laser spectroscopies like coherent Raman scattering and ps photon echoes[79] should prove particularly useful. Besides substitutional impurities, defects created by photodecomposition, or ionizing radiation should be studied. Such experiments are needed to elucidate the size of the defect perturbed domain and the magnitude of the mechanical perturbations introduced by small defects.

Acknowledgment. This research was supported by the US Army Research Office grants DAAL03-G-90-0030 and DAAH04-93-G-0016 to D.D.D., and by the Office of Naval Research, Physics Division grant N00014-89-J-1119 to M.D.F. We gratefully acknowledge many discussions with Prof. Y. Gupta of Washington State University who showed us how to calculate the final temperature after irreversible compression, and several helpful conversations with Dr. Craig Tarver of Lawrence Livermore National Laboratory and Dr. Caryle Storm of Los Alamos National Laboratory.

References and Notes

(1) Coffey, C. S.; Toton, E. T. *J. Chem. Phys.* **1982**, *76*, 949.
(2) Trevino, S. F.; Tsai, D. H. *J. Chem. Phys.* **1984**, *81*, 348.
(3) Zerilli, F. J.; Toton, E. T. *Phys. Rev. B* **1984**, *29*, 5891.
(4) Walker, F. E. *J. Appl. Phys.* **1988**, *63*, 5548.
(5) Dlott, D. D.; Fayer, M. D. *J. Chem. Phys.* **1990**, *92*, 3798.
(6) Wei, T. G.; Wyatt, R. E. *J. Phys. Condens. Matter* **1990**, *2*, 9787.
(7) Lee, E. L.; Green, L. G. Lawrence Livermore Tech. Rept. UCRL-52000-88-1.2, *Energy and Technology Review* Jan-Feb **1988**, 29.
(8) Chapman, D. L. *Phil. Mag.* **1899**, *213*, 47. Jouguet, E. *J. Pure Appl. Math.* **1904**, *70*, 347.
(9) Davis, W. C. *Sci. Am.* **1987**, *256*, 106.

(10) Tarver, C. M. *Combustion and Flame* **1982**, *46*, 157.
(11) Tarver, C.; Calef, D. Lawrence Livermore Tech. Rept. UCRL-52000-88-1.2, *Energy and Technology Review* Jan-Feb **1988**, 1.
(12) Zel'dovich, Y. B.; Raizer, Y. P. *Physics of Shock Waves and High-Temperature Hydrodynamic Phenomena*; Academic Press: New York, 1966.
(13) Zel'dovich, Y. B. *Sov. Phys.-JETP* **1940**, *10*, 542. von Neumann, J. Office of Science Research and Development, Report 549 **1942**. Doering, W. *Ann. Phys.* **1943**, *43*, 421.
(14) Bardo, R. D. *Int. J. Quantum Chem: Quant. Chem. Symp.* **1986**, *20*, 455.
(15) Eyring, H.; Powell, R. E.; Duffrey, G. H.; Darlin, R. B. *Chem. Rev.* **1949**, *45*, 69. Eyring, H. *Science* **1978**, *199*, 740.
(16) Chen, S.; Lee, I.-Y. S.; Tolbert, W. A.; Wen, X.; Dlott, D. D. *J. Phys. Chem.*, in press.
(17) Dlott, D. D. In *Shock Compression in Condensed Matter 1991*; S. C. Schmidt, R. D. Dick and J. W. Forbes, Ed.; Elsevier: New York, 1991; p 709.
(18) Dlott, D. D. *Annu. Rev. Phys. Chem.* **1986**, *37*, 157.
(19) Dlott, D. D. In *Laser Spectroscopy of Solids II*; W. Yen, Ed.; Springer-Verlag: Berlin, 1989.
(20) Wen, X.; Tolbert, W. A.; Dlott, D. D. *Chem. Phys. Lett.* **1992**, *192*, 315.
(21) Dick, J. J.; Mulford, R. N.; Spenser, W. J.; Petit, D. R.; Garcia, E.; Shaw, D. C. *J. Appl. Phys.* **1991**, *70*, 3572.
(22) McGuire, R. R.; Tarver, C. M. In *Proceedings of the Seventh International Symposium on Detonation Processes*, Office of Naval Research: Silver Spring, MD, 1982; p 56.
(23) Mader, C. L. *Numerical Modeling of Detonations*; University of California Press: Berkeley, CA, 1979.
(24) Wight, C. A.; Botcher, T. R. Submitted for publication in *J. Am. Chem. Soc.*
(25) Oyumi, Y.; Brill, T. B. *Combustion and Flame* **1985**, *62*, 213. Brill, T. B.; Oyumi, Y. *J. Phys. Chem.* **1986**, *90*, 6848. Brill, T. B.; Brush, P. J. *Phil. Trans. R. Soc. London, Ser. A* **1992**, *339*, 337.
(26) Johnson, J. N.; Tang, P. K.; Forest, C. A. *J. Appl. Phys.* **1985**, *57*, 4323. Johnson, J. N. *Proc. Roy. Soc. London A* **1987**, *413*, 329. Johnson, J. N. In *Shock Waves in Condensed Matter, 1988*; S. C. Schmidt and N. C. Holmes, Ed.; North-Holland: Amsterdam, 1988; p 527. Karo, A. M.; Hardy, J. R. *J. Phys. (Paris) C* **1987**, *9*, 235.
(27) Bowden, F. P.; Yoffe, A. D. *Fast Reactions in Solids*; Academic Press: New York, 1958.
(28) Campbell, A. W.; Davis, W. C.; Travis, J. R. *Phys. Fluids* **1961**, *4*, 498. Mader, C. L. *Phys. Fluids* **1963**, *6*, 375.
(29) Armstrong, R. W.; Coffey, C. S.; Elban, W. L. *Acta Metall.* **1982**, *30*, 2111. Armstrong, R. W.; Elban, W. L. "Microstructural origins of hot spots in RDX crystals", Chemical Propulsion Information Agency Publication #475, 1987. Coffey, C. S. "Hot Spot Production by Moving Dislocations in a Rapidly Deforming Crystalline Explosive", in Proceedings of the Eighth International Symposium on Detonation, Office of Naval Research, Silver Spring, MD, 1982. Elban, W. L.; Hoffsommer, J. C.; Armstrong, R. W. *J. Mat. Sci.* **1984**, *19*, 552. Frey, R. B. "The Initiation of Explosive Charges by Rapid Shear", in Proceedings of the Eighth International Symposium on Detonation, Office of Naval Research, Silver Spring, MD, 1982.
(30) McGuire, R. R. *Working Group Meeting on the Sensitivity of Explosives*; Center for Technology and Research, New Mexico Institute of Technology, 1987; p 624.
(31) Wilson, W. L.; Wackerle, G.; Fayer, M. D. *J. Chem. Phys.* **1987**, *87*, 2498.
(32) Tsai, D. H. *J. Chem. Phys.* **1991**, *95*, 7497.
(33) Tang, P. K.; Johnson, J. N.; Forest, C. A. In *Proceedings of the Eighth International Symposium on Detonation Processes*, Office of Naval Research: Silver Spring, MD, 1985; p 52.
(34) Kassoy, D. R.; Kapila, A.; Stewart, D. S. *Combust. Sci. Tech.* **1989**, *63*, 33.
(35) Kitaigorodsky, A. I. *Molecular Crystals and Molecules*; Academic Press: New York, 1973.
(36) Pertsin, A. J.; Kitaigorodskii, A. I. *The Atom-Atom Potential Method: Applications to Organic Molecular Solids*; Springer-Verlag: Berlin, 1987.
(37) Warnes, R. H. *J. Chem. Phys.* **1970**, *53*, 1088.
(38) Marsh, S. P., Ed.; *LASL Shock Hugoniot Data*; University of California Press: Berkeley, 1980.
(39) Zeman, S.; Dimun, M.; Truchlik, S. *Thermochim. Acta* **1984**, *78*, 181.
(40) Piermarini, G. J.; Block, S.; Miller, P. J. *J. Phys. Chem.* **1987**, *91*, 3972.
(41) Choi, C. S.; Boutin, H. *Acta Cryst.* **1970**, *16*, 617.
(42) Iqbal, Z.; Bulusu, S.; Autera, J. R. *J. Chem. Phys.* **1974**, *60*, 221.
(43) Prasad, P. A.; Kopelman, R. *J. Chem. Phys.* **1972**, *58*, 5031.
(44) Hoshen, J.; Jortner, J. *J. Chem. Phys.* **1972**, *56*, 993; **1972**, *56*, 5550.
(45) Ziman, J. M. *Models of Disorder*; Cambridge University Press: Cambridge, 1979.
(46) Califano, S.; Schettino, V.; Neto, N. *Lattice Dynamics of Molecular Crystals*; Springer-Verlag: Berlin, 1981.
(47) Nitzan, A.; Jortner, J. *Mol. Phys.* **1973**, *25*, 713. McDonald, J. D. *Ann. Rev. Phys. Chem.* **1979**, *30*, 29. Flynn, G. W. *Acc. Chem. Res.* **1981**, *14*, 334. Parmenter, C. S. *J. Phys. Chem.* **1982**, *86*, 1735.
(48) Kim, H.; Dlott, D. D. *J. Chem. Phys.* **1990**, *93*, 1695.
(49) Hill, J. R.; Dlott, D. D. *J. Chem. Phys.* **1988**, *89*, 842.
(50) Beck, S. M.; Powers, D. E.; Hopkins, J. B.; Smalley, R. E. *J. Chem. Phys.* **1980**, *73*, 2019. Beck, S. M.; Hopkins, J. B.; Powers, D. E.; Smalley, R. E. *J. Chem. Phys.* **1981**, *74*, 43.
(51) Ashcroft, N. W.; Mermin, N. D. *Solid State Physics*; Holt, Reinhart and Winston: New York, 1976.
(52) Hess, L. A.; Prasad, P. N. *J. Chem. Phys.* **1980**, *72*, 573.
(53) Delle Valle, R. G.; Fracassi, P. F.; Righini, R.; Califano, S. *Chem. Phys.* **1983**, *74*, 179.
(54) Righini, R. *Chem. Phys.* **1984**, *84*, 97.
(55) Laubereau, A.; Kaiser, W. *Rev. Mod. Phys.* **1978**, *50*, 608. Elsaesser, T.; Kaiser, W. *Ann. Rev. Phys. Chem.* **1991**, *42*, 83.
(56) Alghren, D. C.; Kopelman, R. *Chem. Phys.* **1980**, *72*, 1.
(57) Dashevsky, V. G. *J. Struct. Chem.* **1965**, *6*, 850; **1966**, *7*, 83.
(58) Nicol, M.; Vernon, M.; Woo, J. T. *J. Chem. Phys.* **1975**, *63*, 1992.
(59) Häfner, W.; Kiefer, W. *J. Chem. Phys.* **1987**, *86*, 4582.
(60) Krishnan, R. S.; Srinivasan, R.; Devanarayanan, S. *Thermal Expansion of Crystals*; Pergamon Press: Oxford, 1979.
(61) Gupta, Y. M., private communication.
(62) Butina, T. A. *Fiz. Goren. Vzr.* **1989**, *25*, 143. Dandache, H. *Solid State Comm.* **1989**, *69*, 667.
(63) Cowperthwaite, M.; Shaw, R. *J. Chem. Phys.* **1970**, *53*, 555.
(64) Van Vleck, J. H. *Phys. Rev.* **1941**, *59*, 730.
(65) Black, J. L.; Halpern, B. I. *Phys. Rev. B* **1977**, *16*, 2879.
(66) Dancz, J.; Rice, S. A. *J. Chem. Phys.* **1977**, *67*, 1418.
(67) McCrone, W. C. *Anal. Chem.* **1950**, *22*, 1225. Fifer, R. A. In *20th JANNAF Combustion Meeting*; 1983; p 581.
(68) Taylor, B. C.; Ervin, L. W. In *Proceedings of the Seventh International Symposium on Detonation Processes*, Office of Naval Research: Silver Spring, MD, 1982; p 3.
(69) Neilson, A. T. In *Working Group Meeting on the Sensitivity of Explosives*; Center for Technology and Research, New Mexico Institute of Technology, 1987; p 56.
(70) Bulusu, S.; Weinstein, D. I.; Autera, J. R.; Velicky, R. W. *J. Phys. Chem.* **1986**, *90*, 4121.
(71) Frank, A. M. In *20th International Conference on High Speed Photography and Photonics*; Victoria, B.C., 1992.
(72) Frank-Kaminetsky, D. A. *Diffusion and Heat Exchange in Chemical Kinetics*; Princeton University Press: Princeton, 1955.
(73) Graham, R. A. *J. Phys. Chem.* **1979**, *83*, 3028.
(74) Eyring, H. *Chem. Eng. News* **1975**, *53*, 27.
(75) White, C. T.; Robertson, D. H.; Elert, M. L. In *Microscopic Simulations of Complex Hydrodynamic Phenomena*; M. Mareschal and B. L. Holian, Ed.; Plenum Press: New York, 1992; p 111.
(76) Chronister, E. L.; Crowell, R. A. *Chem. Phys. Lett.* **1991**, *182*, 27. Crowell, R. A.; Chronister, E. L. *Mol. Cryst. Liq. Cryst.* **1992**, *211*, 361. *J. Phys. Chem.* **1992**, *96*, 1045. *Chem. Phys. Lett.* **1992**, *195*, 602. *J. Phys. Chem.* **1992**, in press.
(77) Prasad, P. N. *Mol. Cryst. Liq. Cryst.* **1979**, *52*, 63.
(78) Lee, I.-Y. S.; Wen, X.; Tolbert, W. A.; Dlott, D. D.; Doxtader, M.; Arnold, D. R. *J. Appl. Phys.*, in press.
(79) Narasimhan, L. R.; Littau, K. A.; Pack, D. W.; Bai, Y. S.; Elschner, A.; Fayer, M. D. *Chem. Rev.* **1990**, *90*, 439. Walsh, C. A.; Berg, M.; Narasimhan, L. R.; Fayer, M. C. *Acc. Chem. Res.* **1987**, *20*, 120.